

Quasiparticle-like peaks, kinks, and electron-phonon coupling at the $(\pi,0)$ regions in the CMR oxide $\text{La}_{2-2x}\text{Sr}_{1+2x}\text{Mn}_2\text{O}_7$

Z. Sun,^{1,2} Y. -D. Chuang,² A. V. Fedorov,² J. F. Douglas,¹ D. Reznik,³ F. Weber,³ N. Aliouane,⁴ D. N. Argyriou,⁴ H. Zheng,⁵ J. F. Mitchell,⁵ T. Kimura,^{6,*} Y. Tokura,⁶ A. Revcolevschi,⁷ and D. S. Dessau^{1,†}

¹*Department of Physics, University of Colorado, Boulder, CO 80309, USA*

²*Advanced Light Source, Lawrence Berkeley National Laboratory, Berkeley, CA 94720, USA*

³*Forschungszentrum Karlsruhe, Institut für Festkörperphysik, Postfach 3640, D-76021 Karlsruhe, German*

⁴*Hahn-Meitner-Institut, Glienicke Str 100, Berlin D-14109, Germany*

⁵*Materials Science Division, Argonne National Laboratory, Argonne, IL 60439, USA*

⁶*Department of Applied Physics, University of Tokyo, Tokyo 113-8656, Japan*

⁷*Laboratoire de Physico-Chimie de l'Etat Solide, University of Paris Sub-11, 91405 Orsay, Cedex, France*

(Dated: December 17, 2018)

Using Angle-Resolved Photoemission (ARPES), we present the first observation of sharp quasiparticle-like peaks in a CMR manganite. We focus on the $(\pi,0)$ regions of k-space and study their electronic scattering rates and dispersion kinks, uncovering the critical energy scales, momentum scales, and strengths of the interactions that renormalize the electrons. To identify these bosons we measured phonon dispersions in the energy range of the kink by inelastic neutron scattering (INS), finding a good match in both energy and momentum to the oxygen bond-stretching phonons.

PACS numbers: 71.18.+y, 71.38.-k, 78.70.Nx, 79.60.-i

The exotic physics in condensed matter systems, such as high temperature superconductivity in cuprates [1] and colossal magnetoresistance (CMR) in manganites [2, 3], is due to strong many-body interactions of unknown origin. Relevant interactions are either electron-electron or electron-boson, where the boson is a collective excitation such as a magnon or, as in the case of conventional superconductivity [4], a phonon. These interactions are typically described as "dressing" the electrons to create quasiparticles, the properties of which determine physical quantities such as electrical and thermal conductivity. In certain cases such as one-dimensional "Luttinger Liquids" [5] and possibly cuprates [6] and manganites [7], the electronic correlations are so strong that the quasiparticle concept falls apart, and only broad and strongly damped electronic excitations have been observed. A side effect of this is that the absence of the quasiparticles gives experimentalists fewer windows into the interactions responsible for the behaviour of the system.

Many-body interactions in manganites are expected to be strong and include the coupling to other electrons plus collective modes such as phonons [8, 9], magnons [10, 11], and orbitons [12, 13]. Although some of these bosonic modes have been extensively studied in the manganites through Raman, X-ray and neutron scattering experiments, the details of how these modes couple to the electrons have been almost completely unexplored. In essence we do not know which modes are most relevant or how strongly they couple to the electrons.

$\text{La}_{2-2x}\text{Sr}_{1+2x}\text{Mn}_2\text{O}_7$ is a naturally layered compound with two MnO_2 planes per unit cell, with the physical properties dominated by these bilayers [14]. The

$x=0.36-0.4$ samples we studied have a transition from a high temperature paramagnetic insulating (PI) state to a low temperature ferromagnetic metallic (FM) state at $T_c \sim 120-130\text{K}$. To uncover the properties of electrons and their interactions with bosonic modes in these compounds, we take advantage of two powerful energy and momentum-resolved techniques, ARPES and inelastic neutron scattering (INS) to individually probe the electrons and bosons throughout the zone, respectively. This powerful combination gives unprecedented clarity into the many-body interactions in the CMR compounds. We observed sharp quasiparticle-like peaks using ARPES, which opens a window for us to study electronic dispersions and scattering rates and how electrons are renormalized by bosonic modes. Phonon dispersions were measured by INS, which have a good match in both energy and momentum to that which should couple to electrons, indicating the relevance of phonons to the interactions in manganites.

The ARPES experiments were performed at beamline 12.0.1 of the Advanced Light Source, Berkeley, using a Scienta SES100 electron spectrometer under a vacuum better than 3×10^{-11} torr. All samples were cleaved *in-situ* at 20 K, and low energy electron diffraction (LEED) patterns confirmed the high quality of the surfaces. The combined instrumental energy resolution of experiments was better than 20 meV and the momentum resolution was about 2 % of the zone edge ($.02 \pi/a$). The neutron scattering experiments were performed on the 1T triple axis spectrometer at the ORPHEE reactor at Saclay utilizing the 220 reflection of copper as the monochromator and the 002 reflection of Pyrolytic graphite. The sample was mounted in a closed-cycle refrigerator with the

measurements performed at 11K.

The electronic spectral function is determined from ARPES data. Fig 1a illustrates the typical Fermi surface of $\text{La}_{2-2x}\text{Sr}_{1+2x}\text{Mn}_2\text{O}_7$ [7]. Theoretically there is a small piece at the zone center consisting of primarily out-of-plane $d_{3z^2-r^2}$ Mn-O states, while the large hole pockets centred at the zone corners are due to bilayer-split in-plane $d_{x^2-y^2}$ Mn-O states [7]. These in-plane states, which are expected to be more important for the transport and magnetic properties of these layered materials, are the focus of this paper. All previous work had been unable to resolve the bilayer splitting. In this work we discovered we could selectively pick up either the bonding or antibonding bands near $(\pi,0)$ regions by tuning the matrix elements, which allows a highly accurate analysis of data. We empirically found that bonding and antibonding portions of the bilayer-split bands are emphasized with 73 eV and 56 eV photons, respectively. The spectral weight at the Fermi energy taken using 56 eV photons at $T=20\text{K}$ is shown in fig 1b, giving a (matrix-element modulated) experimental mapping of the 2D Fermi surface (FS). The weak feature around the zone center as indicated by the red dots in fig 1b is consistent with the prediction of the small electron pocket. Here we focus on data along the blue line in panel a, i.e. the line $(k_x, 0.9\pi/a)$. Fig 1c shows a wide binding energy scan of the antibonding band as a function of k_x at $T=20\text{K}$, exhibiting a clear parabolic dispersive feature with maximal spectral weight around the binding energy 0.4 eV. The bonding band (not shown) has a similar dispersive feature and reaches 400 meV deeper binding energy. The black dots superimposed on the right half of the data show this wide-scale dispersion clearly. Near E_F (below the red arrow) the dispersive feature is sharp and heavily renormalized from the parabolic dispersion, indicating important many-body effects.

An Energy Distribution Curve (EDC) taken at $k=k_F$ from this data (vertical white line in panel c) is plotted in fig 1d. Near E_F there is a clear and well-resolved quasiparticle-like peak [15] - the first such observation in a CMR oxide. This observation by itself has important ramifications for the study of electronic correlations in low dimensional systems such as the layered manganites, as certain important classes of models of correlated electrons [5, 6] require the absence of such quasiparticles. Compared to data on $\text{La}_{2-2x}\text{Sr}_{1+2x}\text{Mn}_2\text{O}_7$ ($x=0.4$) which have very small spectral weight near E_F [7, 16, 17], the appearance of a quasiparticle-like peak is not likely due to improved sample quality issues [17] but rather due to the reduced level of AF-canting [18] in the $x=0.36$ and 0.38 samples, which tends to make these samples electronically more three-dimensional. This trend is consistent with that observed in the cobaltates [19] and ruthenates [20], in which it has been argued that a high dimensionality favors more quasiparticle spectral weight. The overall EDC lineshape shows a peak-dip-hump struc-

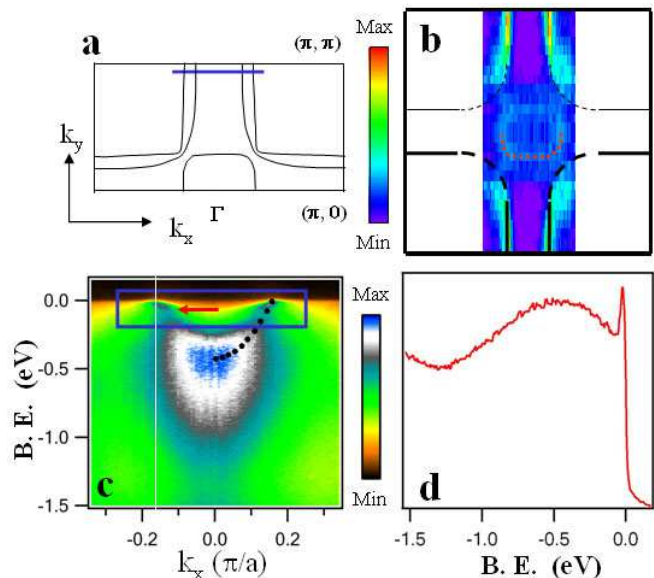


FIG. 1: Low-temperature ($T=20\text{ K}$) ARPES data from $\text{La}_{2-2x}\text{Sr}_{1+2x}\text{Mn}_2\text{O}_7$ ($x=0.38$). (a) A representative Fermi surface, after ref [7]. (b) The spectral weight at E_F over much of the first Brillouin zone and Fermi surfaces of antibonding band (black lines) and $d_{3z^2-r^2}$ Mn-O states (red dots). (c) Binding energy versus momentum (π/a) image plot of the antibonding band from the 0.9π slice (blue line in panel a), with dots determined from a combination of fits to EDCs (deeper energies) and MDCs (near E_F). (d) The EDC at k_F indicated by the vertical white line in (c).

ture (panel d). In the theoretical framework of a Fermi liquid, the hump is the incoherent part of the single particle excitation and can be considered to be "shakeups" of bosonic excitations [7, 8].

The clear presence of quasiparticle-like peaks in the current sample gives us, for the first time, a new and detailed window into the electronic correlations in the manganites. Figure 2 shows details of the near-Fermi energy region of the data. Panel a shows the antibonding data as a function of k_x . The blue points of Panel b show the dispersion relation, which were determined from fits of Momentum Distribution Curves (MDCs) with a Lorentzian lineshape on top of a small monotonically varying background, while the red points show the results from a similar analysis of bonding band data [21] (upper axis - note the different scale from the bottom axis). An s-shaped kink structure, deviating from the non-interacting parabolic dispersion (black dots), can be clearly seen for both bands. These deviations are due to the many-body effects, and in the language of many-body physics are due to the real part of the electron self-energy, $\text{Re}\Sigma$. This kink structure has been observed in $x=0.4$ samples before [22], though we have better statistics now. The slopes of the renormalized and non-interacting dispersions near E_F give the renormalized and bare Fermi

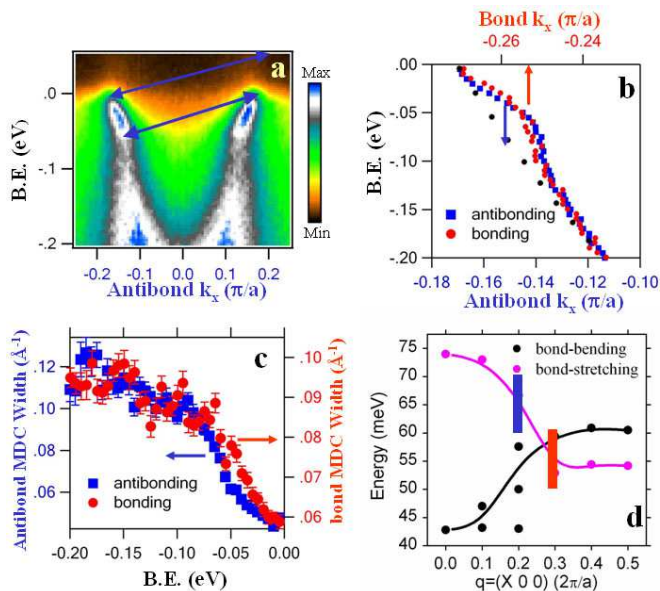


FIG. 2: Electron and phonon dispersion relations and scattering rates. (a) Energy versus momentum image plot of the antibonding electron band from the 0.9π slice (blue frame in figure 1c). (b) MDC derived E vs. k dispersion of antibonding states (blue) and bonding states (red) compared to a parabolic fit to the deeper lying antibonding dispersion (black dots). (c) MDC full widths versus energy for antibonding (blue) and bonding states (red). (d) Phonon dispersion relations from neutron scattering from the bond stretching (pink) and bond bending modes (black) of even symmetry. The bond-bending vibration contributes to multiple modes at some wavevectors because it mixes with other vibrations. The lines are guides to the eye. Electron kink scales and nesting q vectors for the antibonding (blue) and bonding band (red) are also included.

velocities, respectively. In a simple electron-boson coupling model, their ratio can be parameterized as $1+\lambda$, where λ is a measure of the electron-boson coupling strength (also termed the mass enhancement). Since the ratio of the low energy slopes is approximately 2, this would imply $\lambda \sim 1$ for both bonding and antibonding bands. We also note that specific-heat data has indicated similar values of the coupling strengths [23, 24], though this analysis is much less direct as it is based on a comparison to theoretical band structure data. Hence this is the first direct information of coupling parameters in manganites.

Typically, the low temperature metallic state of the manganites is considered to be a rather standard metal without strong correlation effects. The coupling strength λ of the order of unity discovered here tells a different story however. This is in the intermediate-to-strong coupling regime [25], and is on the precipice such that a minor perturbation in parameters giving a small increase in the coupling strength may lead to polaronic localiza-

tion. Therefore these couplings may likely be responsible for the metal-insulator transition which is at the heart of the CMR problem.

The identity of the important boson mode(s) can be determined from these dispersions. Based on the maximum in $\text{Re}\Sigma$ at about 50-60 meV, we estimate the critical energy of the boson mode(s) is around 60-70 meV for the antibonding band and about 50-60 meV for the bonding band [26]. A clear step-increase in the scattering rates centred at the same energy scales are observed (fig. 2c). This self-consistency gives great confidence in the assignment of the critical energy scales to the data. Modes at other energy scales will of course have some relevance as well, but as evidenced by the kink data they will couple to the electrons less strongly than modes near 60 meV.

Various proposals for the important mode coupling in the manganites have been made, including phonons [8, 9], magnons [10, 11], and orbitons [12, 13]. A key point is that the strongly nested Fermi surface should be highly susceptible to a mode with a momentum transfer equal to the nesting vector $q \sim 0.17 \times (2\pi/a, 0)$ for the antibonding band and $q \sim 0.27 \times (2\pi/a, 0)$ for the bonding band. The blue arrow in fig. 2a indicates the corresponding electron scattering within the antibonding band. At these q vectors the excitation energy of magnons is ~ 30 meV [11], and orbitons are larger than 100 meV over the entire zone [13] and so are in disagreement with the critical energy scales we observed here. However, there are longitudinal optical phonons that couple to charge fluctuations in the Mn-O layers exactly in this momentum and energy range, which makes these phonons a good candidate for the dominant coupling.

We performed neutron scattering measurements on $\text{La}_{2-2x}\text{Sr}_{1+2x}\text{Mn}_2\text{O}_7$ ($x=0.4$) to determine the phonon structures and dispersion relations of the longitudinal bond-stretching and bond-bending phonons, as shown in figure 2d. Both even and odd modes with respect to the bilayer structure of $\text{La}_{2-2x}\text{Sr}_{1+2x}\text{Mn}_2\text{O}_7$ have been measured. Only even phonons are shown here - the odd phonons have similar dispersions but are a few meV lower. Overlaid with the phonon dispersion curves on this plot are the kink energy scales from the ARPES data, plotted at the respective q vectors where energy-momentum conservation allows the phonons to scatter from intraband transition (A \rightarrow A (blue), and B \rightarrow B (red)). Interband transitions such as A \rightarrow B will show up at an intermediate position and are not included on the graph. It is seen that both the kink energies and nesting vectors of the electrons match closely with the phonon energies and q values, giving high confidence that it is these phonons which have dominant coupling to the electrons. Especially important are the bond-stretching phonons, which should couple most strongly to the bonding and antibonding electrons (the bond-bending phonons may couple to the bonding electrons as well). The downward dispersion of the bond-stretching phonons also is seen to

match well with the electron kink data, and is in contrast with that found for the upward-dispersive magnons [11]. In fact, the downward dispersion of the bond-stretching phonons has long been considered an anomaly in manganites and other perovskites, as a simple shell-model predicts that the bond-stretch phonons should have an upward dispersion [27]. The downward dispersion is seen to occur at the same q values where the electron nesting occurs, so future studies might consider whether the coupling to the electrons renormalizes these phonon properties as well.

The coupling of electrons to the bond-stretching phonon branch has also been considered to be important in the cuprates. It has been argued that this branch, which has a similar E vs. q relation, may be responsible for electronic dispersion kinks near 70 meV [28], especially in the nodal or (π, π) direction (the antinodal states in the cuprates couple more strongly to a lower energy scale mode such as the B_{1g} phonon [29] or the magnetic resonance mode [30], though the latter coupling is only apparent in the superconducting state). In the cuprates the q value that connects the nodal states does not closely match the q values of the bond-stretch phonon as determined from neutron scattering. This is perhaps the reason why the coupling is in general weaker in the cuprates than in the manganites. The studies of electron-phonon coupling in manganites may provide opportunities to uncover the roles phonons play not only in the CMR effect but also in the pairing of electrons in high- T_c cuprate superconductors.

In summary, we observed sharp quasiparticle-like peaks in $\text{La}_{2-2x}\text{Sr}_{1+2x}\text{Mn}_2\text{O}_7$ using ARPES, which allows us to study how electrons are renormalized by boson modes in manganite. Phonon dispersions were measured by INS, and the bond-stretch phonons have a dispersion closely matching the electronic kinks in both energy and momentum, indicating the important coupling of this phonon branch to electrons in manganites.

We are grateful to T. Devereaux, T. Egami, N. Furukawa, and J. Zhang for helpful discussions. This work was supported by the U.S. Department of Energy under grant DE-FG02-03ER46066 and Contract W-31-109-ENG-38, and by the U.S. National Science Foundation grant DMR 0402814. The ALS is operated by the Department of Energy, Office of Basic Energy Sciences.

* Present address: Los Alamos National Laboratory, Los Alamos, NM 87545, USA

† To whom correspondence should be addressed: Daniel.Dessau@colorado.edu

[1] J. G. Bednorz and K. A. Müller, *Z. Phys. B* **64**, 189 (1986).

- [2] Y. Tokura, Ed. *Colossal Magnetoresistive Oxides, vol. 2 of Advances in Condensed Matter Physics Science* (Gordon and Breach, Amsterdam, 2000).
- [3] T. Chatterji, Ed. *Colossal Magnetoresistive Manganites* (Kluwer Academic Publishers, 2004).
- [4] J. R. Schrieffer, *Theory of superconductivity* (Perseus Books, 1999).
- [5] J. Voit, *Rep. Prog. Phys.* **57**, 977 (1994).
- [6] P. W. Anderson, *The Theory of Superconductivity in the High- T_c Cuprates* (Princeton University Press, 1997).
- [7] D. S. Dessau et al., *Phys. Rev. Lett.* **81**, 192 (1998).
- [8] V. Perebeinos and P. B. Allen, *Phys. Rev. Lett.* **85**, 5178 (2000).
- [9] A. J. Millis et al., *Phys. Rev. Lett.* **74**, 5144 (1995).
- [10] M. Jaime et al., *Phys. Rev. B* **58**, R5901 (1998).
- [11] K. Hirota et al., *Phys. Rev. B* **65**, 64414 (2002).
- [12] J. van den Brink et al., *Phys. Rev. Lett.* **85**, 5174 (2000).
- [13] E. Saitoh et al., *Nature* **410**, 180 (2001).
- [14] J. F. Mitchell et al., *J. Phys. Chem. B* **105**, 10731 (2001).
- [15] We call this peak quasiparticle-like because it is not yet clear if all of the conditions set forth by Landau for true quasiparticles are met, e.g. the peak width scaling quadratically with energy and temperature.
- [16] Y. D. Chuang et al., *Science* **292**, 1509 (2001).
- [17] We have also measured many $\text{La}_{2-2x}\text{Sr}_{1+2x}\text{Mn}_2\text{O}_7$ ($x=0.4$) samples on our same experimental setup, and in contrast to the $x=0.38$ samples we do not observe any signs of quasiparticles at any temperatures, photon energies, or polarizations. Therefore the difference between $x=0.38$ and 0.4 appears to be due to intrinsic issues.
- [18] M. Kubota et al., *J. Phys. Soc. Jpn.* **69**, 1606 (2000).
- [19] T. Valla et al., *Nature* **417**, 627 (2002).
- [20] S. -C. Wang et al., *Phys. Rev. Lett.* **92**, 137002 (2004).
- [21] Bonding band data was from an 0.36 doped sample from which we obtained better statistics, though the same energy scale as from 0.38 data.
- [22] Y. D. Chuang and D. S. Dessau, available at <http://spot.colorado.edu/~dessau/papers/ChatterjiBookv4.pdf>; Y. D. Chuang, thesis, University of Colorado (2001).
- [23] T. Okuda et al., *Phys. Rev. Lett.* **81**, 3203 (1998).
- [24] B. F. Woodfield et al., *Phys. Rev. Lett.* **78**, 3201 (1997).
- [25] G. D. Mahan, *Many Particle Physics*, Chapter 6 (Plenum Press, 1990).
- [26] In the limit of zero broadening we expect the kink energy to asymptotically approach the boson energy scale from below. In the real case with finite signal strength and peak broadening, the kink will never fully approach the boson energy scale and so the kink energy will slightly underestimate the mode energy. We therefore consider the kink energy ~ 60 meV to be the lower limit of the boson energy scale for the antibonding band and ~ 50 meV to be the lower limit for the antibonding band. The upper limit of the boson scale should be about 10 meV greater, where we can clearly distinguish a lone higher energy feature.
- [27] W. Reichardt and M. Braden, *Physica B* **263-264**, 416 (1999).
- [28] A. Lanzara et al., *Nature* **412**, 510 (2000).
- [29] T. Cuk et al., *Phys. Rev. Lett.* **93**, 117003 (2004).
- [30] A. D. Gromko et al., *Phys. Rev. B* **68**, 174520 (2003).